Integrated Ferroelectrics, 123:18–25, 2011

ISSN: 1058-4587 print / 1607-8489 online
DOI: 10.1080/10584587.2011.570591

A Comparative Hybrid DFT Study of Phonons in Several $SrTiO_3$ Phases

EVGENY BLOKHIN,[1,*] DENIS GRYAZNOV,[1,2]
EUGENE KOTOMIN,[1,2] ROBERT EVARESTOV,[3]
AND JOACHIM MAIER[1]

[1]Max-Planck Institute for Solid State Research, Stuttgart, Germany
[2]Institute for Solid State Physics, University of Latvia, Riga, Latvia
[3]Department of Quantum Chemistry, St. Petersburg State University, Peterhof, Russia

Three $SrTiO_3$ phases (cubic, tetragonal antiferrodistortive and tetragonal ferroelectric) are studied at the ab initio *level. Lattice dynamics was calculated via the PBE0 and B3PW hybrid DFT exchange-correlation functionals within the LCAO formalism using the direct frozen-phonon method. The soft-mode-induced phase transitions and thermodynamics (heat capacity and Helmholtz free energy) are discussed. The results obtained are in good agreement with experiments, except for reproduction of the phase transition temperature. The study represents an important first step in considering defective and more complicated perovskite systems.*

Introduction

$SrTiO_3$ (hereafter STO) is a well-known model material for the investigation of mixed conduction [1]. For almost fifty years the low-temperature properties of STO have been an attractive subject for a vast variety of experimental and theoretical studies. The scientific interest in STO could be formally subdivided into two periods. The first wave of interest started in the 60s when an antiferrodistortive (AFD) phase transition near 110 K came into the center of attention [2]. It was shown that the soft phonon mode at the *R*-point of the Brillouin zone (BZ) of a cubic structure associated with a TiO_6-octahedral antiphase rotation is condensed below 110 K resulting in a tetragonal lattice distortion. Additionally a unit cell stretching appears ($c/a > 1$). It should be noted that such lattice instabilities of cubic STO in zero Kelvin calculations have to result in the appearance of imaginary phonon frequencies (see below). The second surge of interest emerged in the 90s when a quantum-stabilized paraelectric regime near 0 K was discovered and an incipient ferroelectric (FE) behavior below 37 K was suggested [3]. An incipient character means that STO has a very large static dielectric response and is only barely stabilized against the condensation of the Γ-point FE soft mode probably by means of quantum fluctuations [3].

Since the 90s *ab initio* calculations started to contribute significantly to the understanding of STO properties. With the development of new computer simulation methods from plane-wave (PW) based DFT-LDA to advanced LCAO-based hybrid DFT schemes,

Received May 20, 2010; in final form July 23, 2010.
*Corresponding author. E-mail: e.blokhin@fkf.mpg.de

the predictive power of theoretical modeling steadily increased and deeper insight into the STO properties became possible. In particular, *ab initio* calculations of the Helmholtz free energy and entropy via phonon contribution are the recent breakthrough that permits calculation of material properties at temperatures above 0 K. The two main techniques for phonon calculations are the direct frozen-phonon (DFP) [4] and the linear-response (LR) [5] methods. Both are completely independent on any experimental data and fitted parameters. Literature applications [6–9] of these methods to cubic STO, however, led to rather inconsistent results concerning the existence of the soft modes at different BZ points (and, if present, whether the obtained frequencies are real or imaginary). First, the PW-LDA calculations performed by Sai and Vanderbilt [6] within the DFP method have shown the concurrent character of the AFD and FE instabilities, *i.e.* hardening of the AFD *R*-phonon and softening of the FE Γ-phonon connected with the volume increase with respect to theoretical equilibrium. Second, the series of the LDA, GGA-PBE and hybrid HSE06 exchange-correlation calculations performed by Wahl and Vogtenhuber [7] via the PW formalism within the DFP method revealed the soft mode at the Γ-point as real for LDA and imaginary for the GGA-PBE and hybrid HSE06 methods. Third, the linear augmented PW-LDA calculations within the LR method performed by LaSota [8] and Lebedev [9] detected imaginary soft modes at the *M*-, *R*- and Γ-points of the BZ. Such a situation is certainly discomforting and this is why it is necessary to apply more accurate LCAO-based hybrid DFT calculations to this problem (to the best of our knowledge, there have been no such attempts so far). Furthermore, a thermodynamic comparison of different STO phases has also never been considered. Thus the present study is intended to make up for these deficiencies. The accurate representation of known physical properties of STO via phonon calculations is necessary before the acquired techniques can be applied to more complex systems. It is important to note that all STO structural transformation effects mentioned above are extremely small and this is why their reproduction could be considered as a sensitive test for the simulation techniques.

Computational Details

In this study the DFP method was chosen for the phonon calculations as it can, unlike the LR method, be used in conjunction with any external code (only the computation of forces is required). We give here only a brief survey emphasizing a computational workflow and some points of specific interest; the detailed method description based on the supercell model can be found *e.g.* in [10].

At the first step the total energy minimization is performed in order to find the equilibrium structure of the crystal. For this purpose we used the CRYSTAL06 computer code [11] (see *ab initio* calculation details below). The equilibrium geometry of the system is defined by the condition that the forces acting on all individual nuclei are equal to zero.

The ground state energy of a crystal is expanded into a Taylor series with respect to atomic displacements (in the harmonic approximation only the terms up to quadratic order in the displacements are retained). In turn, these displacements induce Hellmann-Feynman forces with the phonon frequencies being determined by the eigenvalues of the force matrix, scaled by the nuclear masses. The force summation is performed over the primitive cells inside of the chosen supercell with periodic boundary conditions. One should notice that not every wave vector *k* commensurates with every supercell size, but the general rule is the larger the supercell size, the denser the mapping of the BZ. For a cubic STO we used a supercell consisting of $2 \times 2 \times 2$ primitive cells (40 atoms) since it is small enough to be

calculated in a reasonable time but large enough to be commensurate with all the special *k*-vectors of the corresponding BZ. Similarly for the tetragonal AFD and FE STO supercells consisting of $2 \times 2 \times 2$ primitive cells (80 atoms for AFD and 40 atoms for FE) were adopted. Thus the second step is the construction of the appropriate supercell and displacing of symmetry non-equivalent atoms. We performed this with the aid of the Phonopy code [12] because it allows one to reduce the number of independent displacements to a minimum without dependence on the supercell size, unlike CRYSTAL06, by taking into account both the translational invariance and the full space group of the supercell including inner translations (see details in [10]).

In practice the weak point of the DFP method is the fact that the atomic displacement magnitude is arbitrary and the computer codes implementing this method could produce inconsistent results depending on this magnitude. Generally the displacements should not be too large, so as to preserve the linear relation between forces and displacements. They also should not be too small, so as to avoid numerical noise. Usually a good compromise is obtained with a displacement size on the order of 0.01Å. The default value of the displacement varies depending on computer codes, for example, 0.003Å in CRYSTAL06, 0.01Å in Phonopy, *etc*. In this paper we omit a more detailed discussion of this question.

The third step in the phonon calculation workflow is the calculation of forces induced by displaced atoms. Obviously this should be done using the same code and method as in the first step, otherwise the criterion of equilibrium would not be fulfilled and excess forces would arise.

The fourth step is to use the Phonopy code to calculate symmetrized force constants. After solving the dynamical matrix for different *k*-vectors in the BZ, the eigenvalues (squared phonon frequencies) and eigenvectors (phonon modes) are found. The thermodynamic functions (the Helmholtz free energy and heat capacity) require summations over the phonon eigenvectors in the BZ which can also be done with Phonopy. At this stage finally the temperature is introduced. One should note the general drawback that the mean-field calculations neglect by definition anharmonic effects and this is why calculated temperature dependencies of the Helmholtz free energy and heat capacity are only qualitatively correct (see the results section).

For the *ab initio* calculations of the phonon properties via the CRYSTAL06 computer code we chose the PBE0 [13,14] and B3PW [15] hybrid exchange-correlation functionals, as they had been successfully applied earlier for calculations of bulk and surface perovskite properties [20, 24, 25, 32]. For each functional the corresponding combination of effective core potentials (ECPs) and basis sets was adopted. In the case of the PBE0 functional the CRENBL small-core ECPs [16, 17] were used for Ti and Sr core-valence interactions and the outermost shell basis functions were optimized in order to avoid the basis-set linear dependence known in LCAO crystal calculations. The all-electron 6-311G (*d*) optimized basis set [18] was used for the O atom. In the case of the B3PW the Hay-Wadt small-core ECPs [19] were used for Ti and Sr core-valence interactions and the outermost shell basis functions were taken from Ref. [20] where they had been optimized for the STO bulk crystal. The all-electron 8-411G (*d*) basis set [21] was used for the O atom as it had been adjusted for calculations of crystalline perovskites. The combination of B3PW functional and CRENBL small-core ECPs is considered in our work [33]. The Monkhorst–Pack [22] scheme of the $8 \times 8 \times 8$ k-point mesh in the BZ was applied and accurate tolerances were used for the Coulomb and exchange integral calculations (values 8 8 8 8 16 in CRYSTAL06). The tolerance of the energy convergence on the self-consistent field (SCF) cycles was set to 10^{-10} a.u. Additionally the DFT density and grid weight tolerances were increased (values 8 and 16 in CRYSTAL06) and an extra-large pruned DFT integration grid was adopted.

Table 1
$SrTiO_3$ bulk properties.

Property	PW, VASP code [7] HSE06	LCAO, CRYSTAL code, this work B3PW Hay-Wadt	LCAO, CRYSTAL code, this work PBE0 CRENBL	Expt.
Cubic				
Lattice constant, Å	3.90	3.91	3.91	3.91[26]
Direct band gap, eV	3.47	4.00	4.24	3.75[27]
Bulk modulus, GPa	192	193	195	179[28]
Tetragonal AFD				
Ratio *c/a*	1.0010	1.0013	1.0011	1.0009 (10 K)[29]
TiO_6 rotation angle, °	2.6	1.1	0.9	2.1 (4 K)[2]

Results and Discussion

In theory the knowledge of soft phonon mode symmetry of the initial structure allows the prediction of the possible symmetry of the derivative structure (*e.g.,* using Stokes and Hatch tables [23]). In particular the soft phonon at the *R*-point of the BZ of a cubic (*Pm-3m*) structure in the case of STO induces the tetragonal AFD (*I4/mcm*) structure (this was proved by experiments, see introduction), whereas the soft phonon at the Γ-point could induce the tetragonal FE (*P4mm*) structure.

In this study the phonon spectra of these three structures of STO are considered. However, the latter structure is taken into account only for a comparison as a model FE phase because a real FE phase tends to condense from the tetragonal AFD phase.

Since the phonon properties were computed for the equilibrium structure, the bulk properties of STO were obtained and considered for preliminary comparison. In Table 1 we sum up the results for the PBE0, B3PW (LCAO formalism) and HSE06 [7] (PW formalism, the range-separated variant [7] of the PBE0). As can be seen, there is a good agreement with experiment (though the rotational angle of the AFD phase is slightly off) confirming the fact that hybrid DFT functionals treat crystalline bulk properties accurately [20, 24]. Interestingly, the smaller the calculated band gap of the cubic phase the larger the calculated octahedral rotational angle of the tetragonal AFD phase (this effect was also noted in [24]). Both the hybrid functionals PBE0 and B3PW reproduce the total energy gain of the tetragonal AFD and FE phases with respect to the cubic phase (though the energy difference is extremely small, in the range of meV). However, in the case of phonon properties, a distinction arises between the PBE0 and B3PW-based calculations.

In temperature-induced phase transitions the anharmonicity effects play a fundamental role: harmonic calculations generally yield an imaginary frequency for the soft mode at 0 K whereas at higher temperatures anharmonicity stabilizes the soft mode. This is why the comparison of the calculated soft mode frequencies with experiment can be problematic. It is seen (Table 2) that the PBE0 and B3PW functionals treat the soft modes in STO differently, predicting real and imaginary frequencies respectively. By contrast, hard modes remain similar and the harder the mode the better the agreement with experiment. The same situation in general persists for the soft and hard modes of the tetragonal AFD and FE phases, suggesting that a careful comparison of functionals needs to be done. As

Table 2
Phonon frequencies in a cubic phase of $SrTiO_3$ (cm^{-1}).

		LCAO, CRYSTAL Phonopy codes		
BZ point	PW, VASP code [7] HSE06	B3PW Hay-Wadt	PBE0 CRENBL	Exp. (297 K)[30]
Γ	***74i***	***112i***	16	91
	162	160	180	170
	250	257	267	265
	533	539	547	547
R	***∼80i***	***43i***	63	52
		140	153	145
		446	459	446
		454	463	450
		467	468	474

consequence of this, the thermodynamic functions for the PBE0 and B3PW (Figs. 1 and 2) differ because imaginary modes in the case of B3PW are neglected and do not contribute to the summation (it is performed over real frequencies only). Apparently this affects the results when comparing the calculated thermodynamic functions to experiment. For the heat capacity the agreement with the experiment [31] at 90–180 K is better for the PBE0

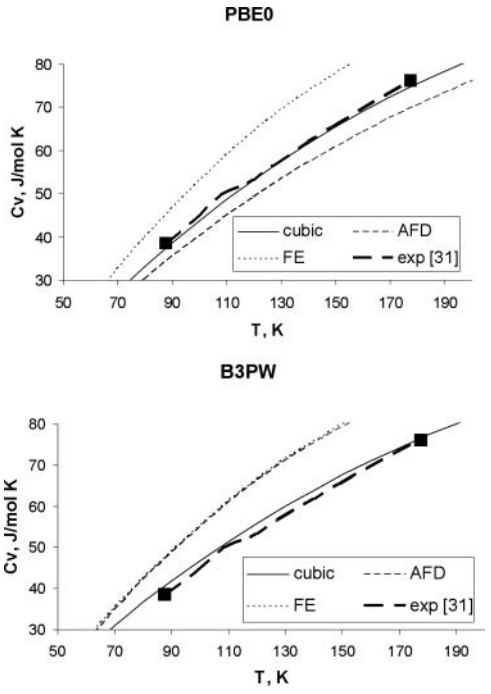

Figure 1. Calculated heat capacity of $SrTiO_3$ (J/mol K).

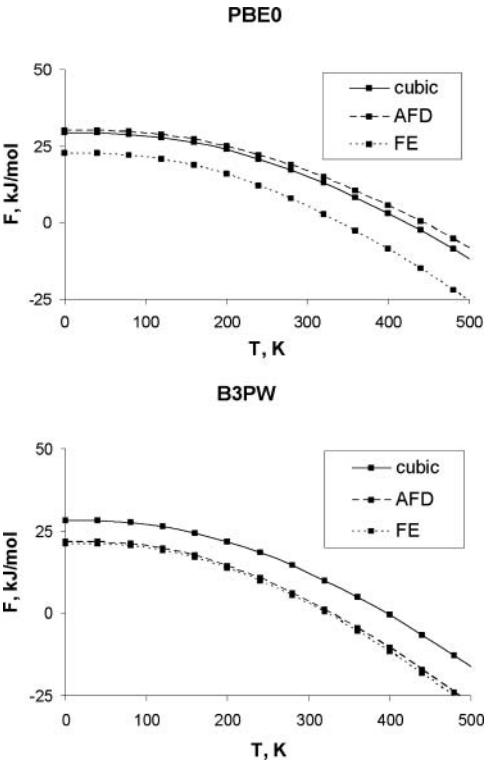

Figure 2. Calculated Helmholtz free energy of $SrTiO_3$ (kJ/mol).

than for the B3PW. The B3PW functional shows a noticeable energetic preference for the AFD phase with respect to the cubic one over the whole temperature range considered. For the PBE0 at temperatures $T < 110$ K the Helmholtz free energy gain tends to disappear (the difference does not exceed several meV), but above 110 K the cubic STO Helmholtz free energy is distinctly lower (*e.g.* more than 0.02 eV at room temperature), in agreement with experiment.

The imaginary frequencies observed in the case of the B3PW functional confirm the presence of the AFD phase transition, but they also complicate correct calculations of the thermodynamic functions as their contribution is ignored. Additionally, the results from the B3PW and HSE06 [7] agree concerning the presence of imaginary frequencies. Furthermore, while choosing between two combinations of functionals, ECPs and basis sets used in this study, one has to take into account that the PBE0/CRENBL requires on average twice much computation time than the B3PW/Hay-Wadt.

The FE phase considered in this study is simplified since the TiO_6-octahedra rotation is neglected. In this case one should expect an occurrence of the AFD soft mode. This rotational mode is soft indeed (imaginary for the B3PW and real for the PBE0), being split into A_2 and E modes (depending on which particular FE displaced oxygen atoms are involved with the rotational motion). In the tetragonal AFD phase the soft FE E_u and A_{2u} modes are found to be imaginary for the B3PW (confirming the results by Sai and Vanderbilt [6]) but real for the PBE0.

Summary

1. The hybrid DFT PBE0 and B3PW functionals respectively combined with CRENBL and Hay-Wadt ECPs and basis sets within the LCAO formalism are both shown to accurately reproduce the electronic and phonon properties of STO. However they diverse in describing the soft phonon modes, resulting in either real or imaginary frequencies respectively, thus contributing differently to the thermodynamics.
2. Experimentally known low temperature Γ- and R-phonon instabilities are reproduced in the cubic STO. In the tetragonal AFD phase the FE soft mode split into E_u and A_{2u} modes is detected. In turn, in the tetragonal FE phase the AFD soft mode split into A_2 and E modes is detected.
3. A comparison of the heat capacities and Helmholtz free energies vs. temperature is performed *ab initio* for the first time for three different STO phases. The experimentally measured heat capacity between 90 and 180 K is reproduced for both functionals. For the B3PW the gain in Helmholtz free energy of the tetragonal AFD phase with respect to the cubic phase obtained though the experimental temperature dependence is not reproduced. For the PBE0 the temperature correlation tends to be present but the gain in Helmholtz free energy tends to be absent.

Acknowledgment

This study was partly supported by EURO-NET MATERA project.

References

1. R. Merkle and J. Maier, How is oxygen incorporated into oxides? A comprehensive kinetic study of a simple solid-state reaction with $SrTiO_3$ as a model material. *Angew. Chem. Int. Ed.* **47**, 3874–3894 (2008).
2. H. Unoki and T. Sakudo, Electron spin resonance of Fe^{3+} in $SrTiO_3$ with special reference to the 110°K phase transition. *J. Phys. Soc. Japan* **23**, 546–552 (1967).
3. K. A. Müller, W. Berlinger, and E. Tosatti, Indication for a novel phase in the quantum paraelectric regime of $SrTiO_3$. *Z. Phys. B.–Cond. Matt.* **84**, 277–283 (1991).
4. K. Parlinski, Z. Li, and Y. Kawazoe, First-principles determination of the soft mode in cubic ZrO_2. *Phys. Rev. Lett.* **78**, 4063–4066 (1997).
5. S. Baroni, P. Giannozzi, and A. Testa, Green's-function approach to linear response in solids. *Phys. Rev. Lett.* **58**, 1861–1864 (1987).
6. N. Sai and D. Vanderbilt, First-principles study of ferroelectric and antiferrodistortive instabilities in tetragonal $SrTiO_3$. *Phys. Rev. B.* **62**, 13942 (2000).
7. R. Wahl, D. Vogtenhuber, and G. Kresse, $SrTiO_3$ and $BaTiO_3$ revisited using the projector augmented wave method: Performance of hybrid and semilocal functionals. *Phys. Rev. B.* **78**, 104116 (2008).
8. C. Lasota, C. Wang, R. Yu, and H. Krakauer, Ab initio linear response study of $SrTiO_3$. *Ferroelectrics* **194**, 109–118 (1997).
9. A. Lebedev, Ab initio calculations of phonon spectra in $ATiO_3$ perovskite crystals (A = Ca, Sr, Ba, Ra, Cd, Zn, Mg, Ge, Sn, Pb). *Physics of the Solid State* **51**, 362–372 (2009).
10. R. A. Evarestov and M. V. Losev, All-electron LCAO calculations of the LiF crystal phonon spectrum: Influence of the basis set, the exchange-correlation functional, and the supercell size. *J. Comput. Chem.* **30**, 2645–2655 (2009).
11. R. Dovesi, V. R. Saunders, C. Roetti, R. Orlando, C. M. Zicovich-Wilson, F. Pascale, B. Civalleri, K. Doll, N. M. Harrison, I. J. Bush, Ph. D'Arco, and M. Llunell, CRYSTAL06 User's Manual, University of Torino, Torino, 2008.

12. A. Togo, F. Oba, and I. Tanaka, First-principles calculations of the ferroelastic transition between rutile-type and $CaCl_2$-type SiO_2 at high pressures. *Phys. Rev. B.* **78**, 134106-1-9 (2008).
13. J. P. Perdew, M. Ernzerhof, and K. Burke, Rationale for mixing exact exchange with density functional approximations. *J. Chem. Phys.* **105**, 9982–9985 (1996).
14. M. Ernzerhof and G. E. Scuseria, Assessment of the Perdew-Burke-Ernzerhof exchange-correlation functional. *J. Chem. Phys.* **110**, 5029–5036 (1999).
15. A. D. Becke, Density-functional thermochemistry. III. The role of exact exchange. *J. Chem. Phys.* **98**, 5648–5652 (1993).
16. M. M. Hurley, L. F. Pacios, P. A. Christiansen, R. B. Ross, and W. C. Ermler, Ab initio relativistic effective potentials with spin-orbit operators. II. K through Kr. *J. Chem. Phys.* **84**, 6840–6853 (1986).
17. L. A. LaJohn, P. A. Christiansen, R. B. Ross, T. Atashroo, and W. C. Ermler, Ab initio relativistic effective potentials with spin–orbit operators. III. Rb through Xe. *J. Chem. Phys.* **87**, 2812–2824 (1987).
18. R. Krishnan, J. S. Binkley, R. Seeger, and J. A. Pople, Self-consistent molecular orbital methods. XX. A basis set for correlated wave functions. *J. Chem. Phys.* **72**, 650–654 (1980).
19. P. J. Hay and W. R. Wadt, Ab initio effective core potentials for molecular calculations. Potentials for the transition metal atoms Sc to Hg. Potentials for main group elements Na to Bi. Potentials for K to Au including the outermost core orbitals. *J. Chem. Phys.* **82**, 270–310 (1984).
20. S. Piskunov, E. Heifets, R. I. Eglitis, and G. Borstel, Bulk properties and electronic structure of $SrTiO_3$, $BaTiO_3$, $PbTiO_3$ perovskites: An ab initio HF/DFT study. *Comput. Mater. Sci.* **29**, 165–178 (2004).
21. T. Bredow, K. Jug, and R. Evarestov, Electronic and magnetic structure of $ScMnO_3$. *Phys. Stat. Sol. (b)* **243**, R10–R12 (2006).
22. H. J. Monkhorst and J. D. Pack, Special points for Brillouine-zone integrations. *Phys. Rev. B* **13**, 5188–5192 (1976).
23. H. T. Stokes and D. M. Hatch, Isotropy Subgroups of the 230 Crystallographic Space Groups, Singapore: World Scientific, 1988.
24. E. Heifets, E. Kotomin, and E. Trepakov, Calculations for antiferrodistortive phase of $SrTiO_3$ perovskite: Hybrid density functional study. *J. Phys.Cond. Matt.* **18**, 4845–4851 (2006).
25. R. A. Evarestov, Quantum Chemistry of Solids. The LCAO First Principles Treatment of Crystals. Springer Series in Solid State Sciences, Vol. 153. Heidelberg: Springer; 2007.
26. L. Cao, E. Sozontov, and J. Zegenhagen, Cubic to tetragonal phase transition of $SrTiO_3$ under epitaxial stress: An x-ray backscattering study. *Phys. Stat. Solidi A* **181**, 387–404 (2000).
27. K. Van Benthem, C. Elsaesser, and R. H. French, Bulk electronic structure of $SrTiO_3$: Experiment and theory. *J. Appl. Phys.* **90**, 6156–6164 (2001).
28. Ferroelectrics and Related Substances, edited by K. H. Hellwege and A. M. Hellwege, *Landolt-Börnstein, NewSeries, Group III*, Vol. 3, Berlin: Springer-Verlag, 1969.
29. A. Heidemann and H. Wettengel, Die Messung der Gitterparameteränderung von $SrTiO_3$. *Z. Phys.* **258**, 429–438 (1973).
30. W. G. Stirling, Neutron inelastic scattering study of the lattice dynamics of strontium titanate: Harmonic models. *J. Phys. C: Solid State Phys.* **5**, 2711–2730 (1972).
31. I. Hatta, Y. Shiroishi, K. A. Müller, and W. Berlinger, Critical behavior of the heat capacity in SrTiO3. *Phys. Rev. B.* **16**, 1138–1145 (1977).
32. R. I. Eglitis and D. Vanderbilt, First-principles calculations of atomic and electronic structure of $SrTiO_3$ (001) and (011) surfaces. *Phys. Rev. B.* **77**, 195408 (2008).
33. R. A. Evarestov, E. Blokhin, D. Gryaznov, E. A. Kotomin, and J. Maier, Phonon calculations in cubic and tetragonal phases of $SrTio_3$: A comparative LCAO and plane wave study. *Phys. Rev. B.* **83**, 134108-1-9 (2011).